Confronting Socioeconomic Racism in the Context of Urban Flooding in the Northeast

Abstract:

This study quantifies flood exposure across historical HOLC redlining zones in New York City using Sentinel-1 SAR imagery and Google Earth Engine. We analyzed six heavy-rainfall events (2018–2021) and projected future risk under moderate and extreme scenarios from the NYC Stormwater Resiliency Plan. “Hazardous” neighborhoods exhibited 2.30–4.40% flooded pixels per event—about double the 0.99–1.51% in “Best” areas—and face over fourfold higher future flood exposure. Flood prevalence positively correlates with social vulnerability and crime rates and inversely with household income. These findings underscore enduring socieconomic racism and the need for equity-focused climate resilience planning.

Key words: Environmental racism, urban flooding, historical redlining, Sentinel-1 SAR, Google Earth Engine, Social Vulnerability Index, climate resiliency, socioeconomic disparities.

Table of Contents:

1. Introduction

Geography of New York City

Located in the northeastern United States, New York City is one of the most populous and diverse cities in the entire world. In fact, more than eight million people live across the five boroughs of the Bronx, Brooklyn, Manhattan, Queens, and Staten Island. Urbanization over the past centuries has replaced natural permeable surfaces with roads, buildings, roofs and other impervious surfaces — increasing flood intensity in urban areas (Pielke and Downton, 2000). Importantly, New York City is located on the coast in a region that is subject to severe precipitation events that can cause both coastal and inland street flooding (González et al., 2019). As Earth's climate continues to change, storm events are predicted to intensify, putting areas such as New York City at greater risk of severe flooding disasters (NCA 2018). Since the twentieth century, there has been an increasing trend towards more extreme precipitation in New York City. In fact, the upper range of regional precipitation is expected to increase by approximately 10% by the 2020s, 13% by the 2050s, 19% by the 2080s, and 25% by 2100 (Horton et al., 2015).

History of Redlining

Redlining was a process that was systematically implemented in the United States to prohibit minority populations from receiving loans to buy houses in majority-white neighborhoods that were meant to be preserved as "safe." Between 1935 and 1940, the Home Owners' Loan Corporation (HOLC), established as part of President Franklin D. Roosevelt's New Deal, created color-coded maps for major cities all across America. Within each map, every residential

neighborhood would receive a grade: 'A' corresponded to a ranking of “Best” and the color green, 'B' corresponded to a ranking of “Still Desirable” and the color blue, 'C' corresponded to a ranking of “Definitely Declining” and the color yellow, and 'D' corresponded to a ranking of “Hazardous” and the color red.

As displayed in Figure 1, New York City was one of the cities included in the residential security map survey. In a trend seen across the entire nation, the majority of black and low-income households were concentrated within heavily redlined areas due to the history of discrimination that restricted them to residing in economically-disadvantaged communities. Even today, black homeowners are five times as likely to own real estate in formerly redlined neighborhoods than greenlined ones (Lerner, 2020). In consequence, the practice of redlining effectively served to clasp the framework of inequality in place (Fishback et al., 2020). In this paper, geospatial data for the redlining maps created by the Home Owners’ Loan Corporation were digitally provided by *Mapping Inequality* (Nelson et al., 2021).

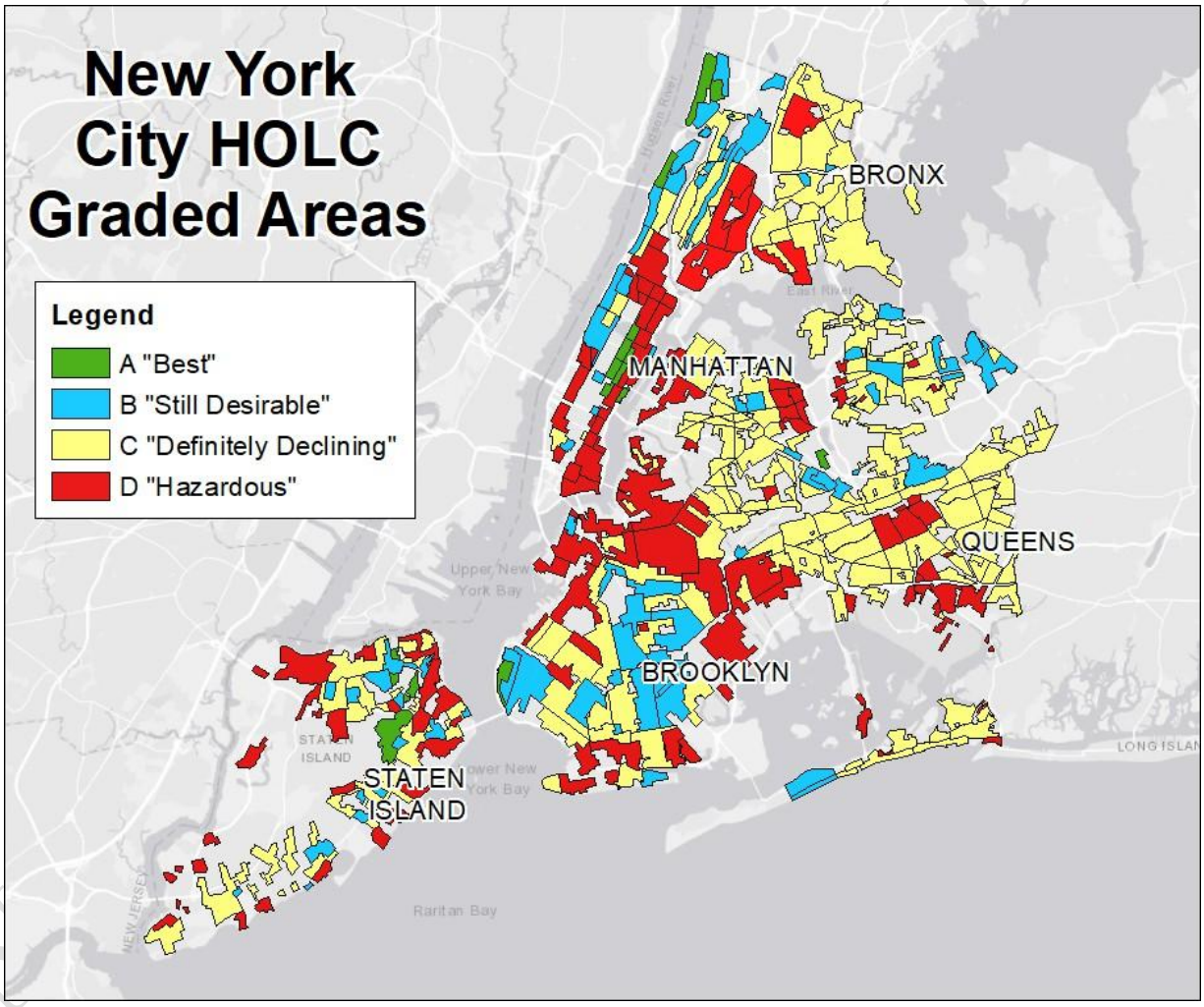

Figure 1: The spatial distribution of HOLC graded areas in New York City for the four-category rating system using geospatial data generated by *Mapping Inequality*.

Earth Observation Applications

Remote sensing is the acquisition of information about an object and its environment from a distance. In the case of Earth observations, remote sensing often takes place in the form of satellite measurements that can cover large spatial and temporal scopes at a relatively low cost.

While there are many applications utilizing remote sensing for monitoring flood extent, multiple challenges can arise that include data accessibility, temporal resolution, and delineating flood boundaries — differentiating water pixels from land pixels when examining the boundary where they meet (Schumann et al., 2009). All these challenges are magnified when attempting to detect water pixels on the diverse terrain of urban environments like New York City, which oftentimes includes multiple surface types concentrated in a single area (Acharya et al., 2018). Previous studies have also shown that the use of widely applied indices such as the Normalized Difference Vegetation Index (NDVI) do not perform well for monitoring flood extent in urban environments. In response, progress has been made in developing indices that are more specific to this type of application, such as the Modified Normalized Difference Water Index (MNDWI), which can enhance the detection of water features and suppress noise from the built environment (Xu, 2006). However, given the unique urban landscape of major metropolitan areas, these indices also face the challenge of varying surface types. Therefore, this paper endeavors to address the gap facing the remote sensing field in the detection of flooded areas in urban settings.

Remote sensing has also been previously utilized alongside redlining data to determine the extent to which redlined areas face an increase in vulnerability to the impacts of climate change. A recent research study reported that 94% of the redlined areas experienced greater land surface temperatures than non-redlined neighborhoods, with the national average showing that land surface temperatures in redlined areas are approximately 2.6°C warmer than non-redlined areas (Hoffman et al., 2020). Similar results from corresponding studies also show the strong correlation between redlined areas and higher land surface temperatures on a regional scale (Li et al., 2021, Saverino et al., 2021, Wilson, 2020). Nevertheless, flood detection from remote sensing has never been utilized before in conjunction with redlining data to quantify the magnitude of present-day environmental racism. Consequently, this paper also serves to lead the environmental justice field in determining whether redlined areas are more vulnerable to flooding events than non-redlined areas.

In the next section, a novel methodology is introduced using a combination of remote sensing and in-situ data that can effectively classify and extract flood pixels after large precipitation events. The conditions of each HOLC area are then compared with one another to determine if there are significant differences detected in the amount of exposure to urban flooding between the four categories of “Best,” “Still Desirable,” “Definitely Declining,” and “Hazardous.”

What began as an urban planning strategy to determine locations ideal for the security of home loans during the Great Depression has potentially placed millions of Americans more at risk of exposure to climate hazards.

2. Methodology

Urban Flooding Workflow

The urban flooding analysis in New York City involves two distinct scenarios for assessing risk in redlined areas: (1) Current Flood Risk (2) Future Flood Risk. Figure 2 summarizes the research workflow that was followed for both scenarios.

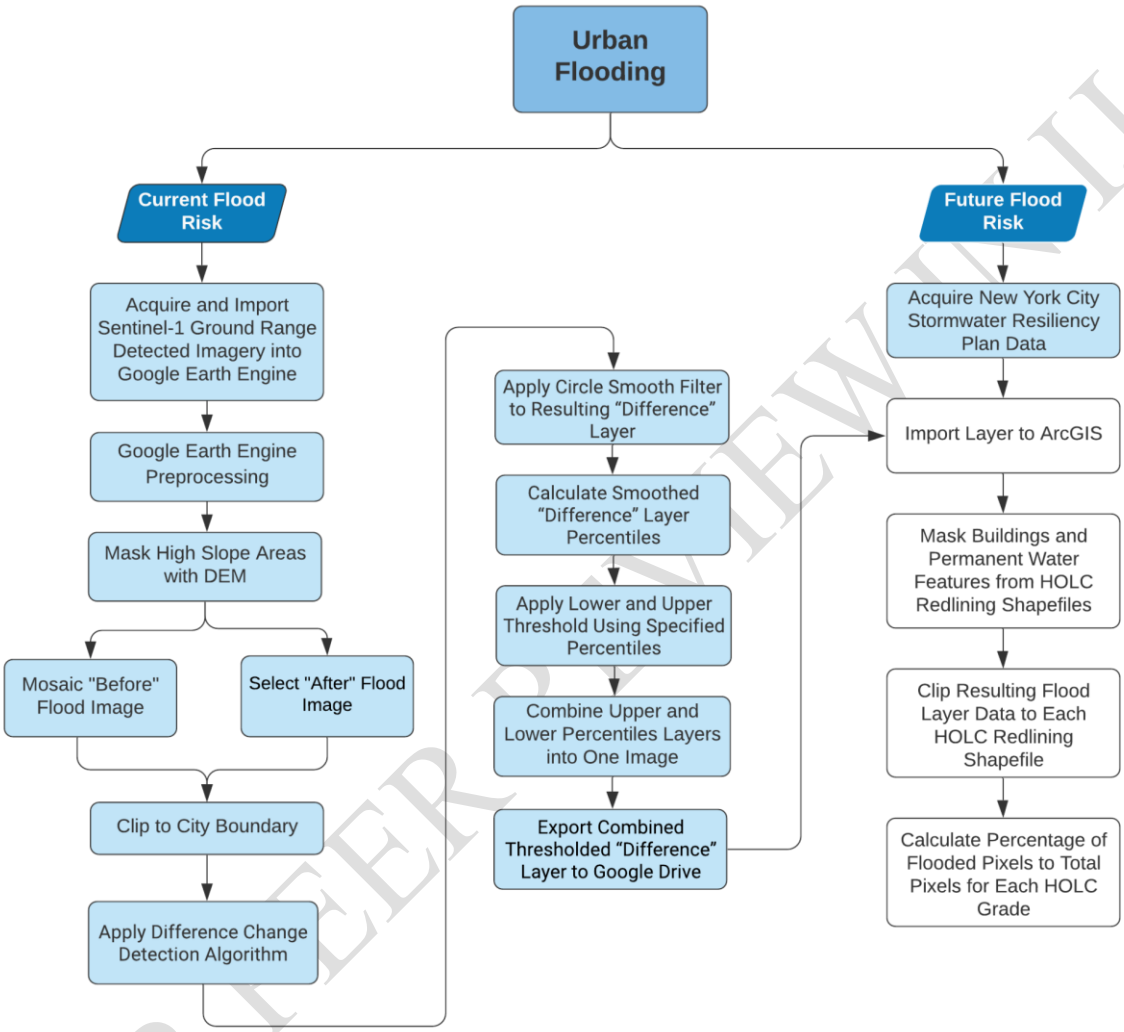

Figure 2: The research workflow utilized for assessing both current flood risk and future flood risk for each of the HOLC graded areas in New York City.

Current Flood Risk

Remote sensing data from the European Space Agency's Sentinel-1 Satellite was used for quantifying the extent of current flood risk. In particular, the study took advantage of the synthetic-aperture radar (SAR) aboard Sentinel-1 that produces an energy signal and then records the amount of energy reflected back to the radar system in order to generate two-dimensional images of the Earth's surface. The main benefit of utilizing SAR data was that the system functioned in nearly all weather conditions, which became especially helpful for analyzing precipitation events that brought heavy cloud coverage in the sky.

In order to identify days for potential flood events, data from ground-based weather stations were accessed throughout New York City to collect precipitation data from the National Oceanic and Atmospheric Administration (NOAA) Climate Data Online Database. In total, there were sixteen local stations available for the analysis, with at least one station in each borough. For each of the weather stations, dates were identified that had one inch or greater of total accumulated precipitation. Figure 3 displays one of the sixteen stations that was considered for the analysis.

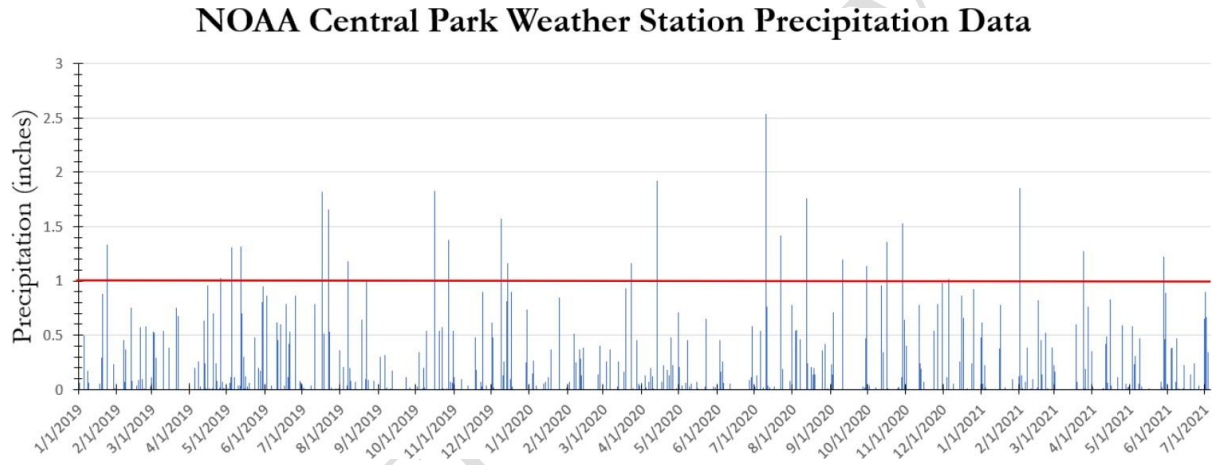

Figure 3: The Central Park Weather Station precipitation data acquired from NOAA Climate Data Online. A threshold of at least one inch of precipitation was set for the analysis, as delineated with all values above the red line. The complementary fifteen weather stations are denominated by the following identifications: Bronx 1.5 NE, Brooklyn 3.1 NW, Howard Beach 0.4 NNW, Jackson Heights 0.3 WSW, JFK International Airport, LaGuardia Airport, Middle Village 0.5 SW, New York 8.8 N, Queens 2.1 NE, Queens 3.4 NNW, Queens 3.7 N, Queens 4.7 SW, Staten Island 1.4 SE, Staten Island 4.5 SSE, and Stuyvesant Square Park 4.9 NNW.

All dates identified as having one inch or more of accumulated precipitation from the weather station data were matched with Sentinel-1 imagery from the Alaska Satellite Facility. In total, forty-one Sentinel-1 snapshots matched with the initial search criteria. Along with rainfall, however, the precipitation levels measured by the local weather stations from NOAA Climate Data Online also took into account precipitation from snowfall. Therefore, in order to validate the presence of urban flooding, each date was subsequently cross-referenced with information from the National Weather Service and local news articles detailing reports of flash flooding events in New York City. After the aforementioned secondary search was completed, six Sentinel-1 snapshots remained and were categorized as the post-flooding images.

Additionally, the analysis also applied imagery that represented baseline conditions without precipitation. In order to perform this step, NOAA Climate Data Online was utilized to identify dates that had zero inches rainfall. Based on this criteria, forty-three Sentinel-1 images were pinpointed and categorized as the pre-flooding images.

From there, I coded a program in Google Earth Engine with JavaScript that could automatically classify pixels as either flooded or non-flooded. To begin with, each Sentinel-1 image was imported into Google Earth Engine, where it was automatically preprocessed with GRD border noise removal, thermal noise removal, radiometric calibration, and terrain correction. In order to refine the initial raster data, areas of high slope, as calculated from a digital elevation model of New York City, were masked out of each image.

Following all the image preprocessing, the forty-three pre-flooding images were mosaiced together by the mean value of each overlapping pixel and afterwards clipped to a boundary shapefile of New York City. Each of the six post-flooding images were also clipped to the same boundary shapefile of New York City. Afterwards, a backscatter change detection algorithm between each of the six post-flooding images and the single mosaiced pre-flooding image was executed, resulting in a difference layer. Once a circle smooth filter of twenty-five meters was applied to remove potential speckles in the data, the script then calculated the percentiles of pixel values within the difference layer.

In order to validate and determine the specific threshold associated with flooded or non-flooded pixels, images and videos from social media were incorporated into the analysis as in-situ data to assess the specific areas where flooding was known to have occurred. After geotagging the exact location of where each social media post took place, the surrounding reflectance values from the SAR satellite signal were collected and compared amongst the other flooding locations.

Figure 4: Screenshots of flooded streets in New York City that were collected from various social media platforms and incorporated into the analysis as a source of in-situ data to verify areas where flooding was known to have occurred.

Using the difference layer, a threshold criteria was applied for values within two standard deviations (i.e., less than the 5th percentile or greater than the 95th percentile) to be marked as flooded. Extreme values displaying flooded pixels were marked with a value of 1 and highlighted in dark blue, while all other values within two standard deviations, the non-flooded areas, were marked with a value of 0. After the threshold was applied to all six post-flooding images, they were subsequently exported from Google Earth Engine and imported into ArcGIS. Figure 5 shows the main inputs and outputs from the Google Earth Engine algorithm.

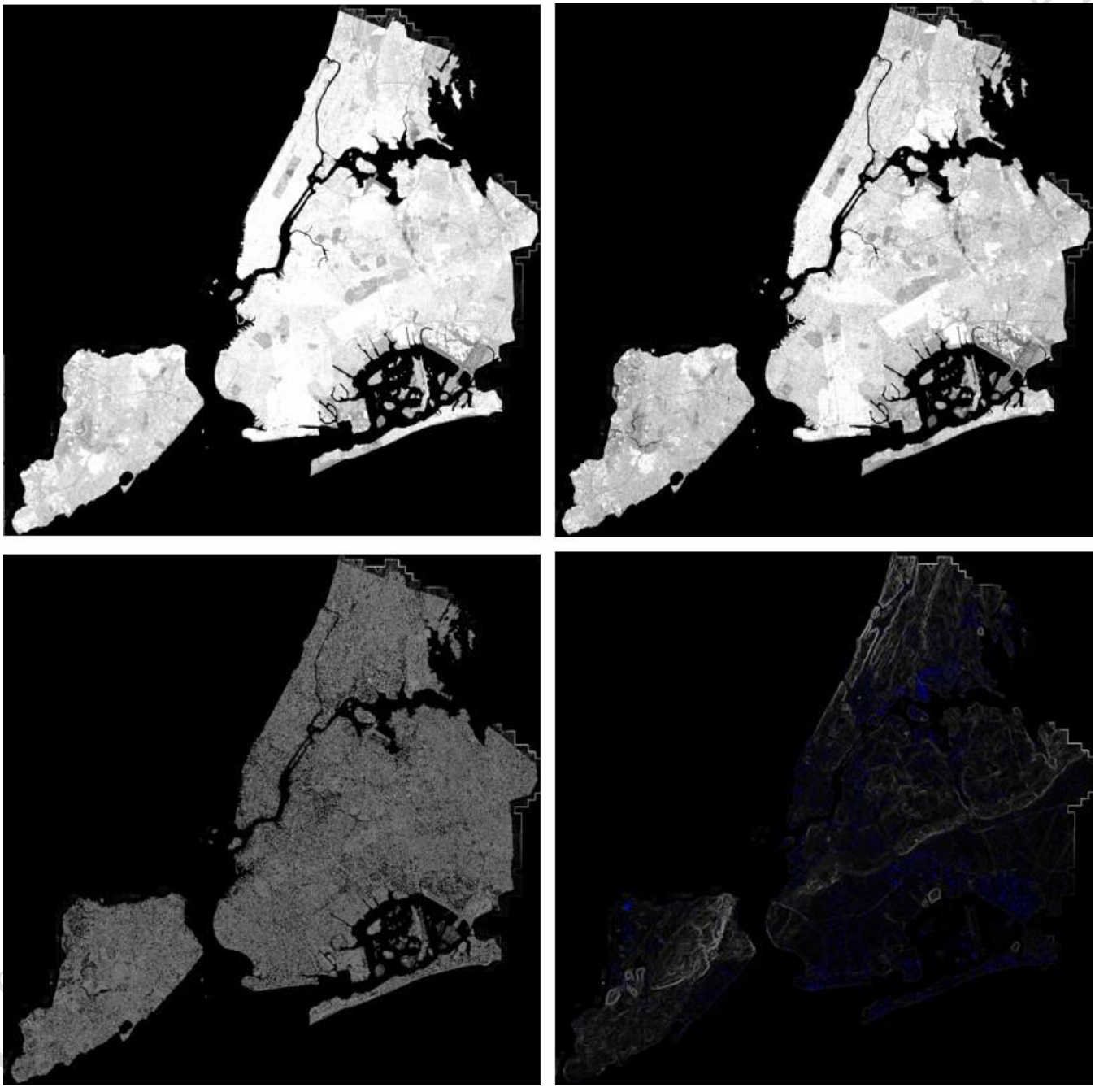

Figure 5: The Sentinel-1 SAR data layers used as inputs and outputs to classify flooded pixels in NYC. The images in the college include top left: a mosaic of forty-three Sentinel-1 SAR images that represent days with no precipitation (the pre-flooding image, top right: an image captured on August 11th, 2018 after flooding in New York City that exceeded one inch of accumulated rainfall (the post-flooding image), bottom left: the smoothed difference between the pre-flooding image and post-flooding image layers, bottom right: the areas highlighted in dark blue that were classified as flooded pixels based on Google Earth Engine algorithm.

Future Flood Risk

The percentage of each redlining grade at risk of future flooding was determined using a dataset provided from the City of New York Stormwater Resiliency Plan, which was created by urban planners with extensive knowledge of New York City's existing drainage system (New York Mayor's Office of Resiliency, 2019). Moderate flood risk is defined as two inches of rain falling in one hour combined with 2.5 feet of sea level rise. Extreme flooding is defined as approximately 3.5 inches of rain falling in one hour combined with 4.8 feet of sea-level rise. A selection of the New York City Stormwater Flood Map is presented in Figure 6.

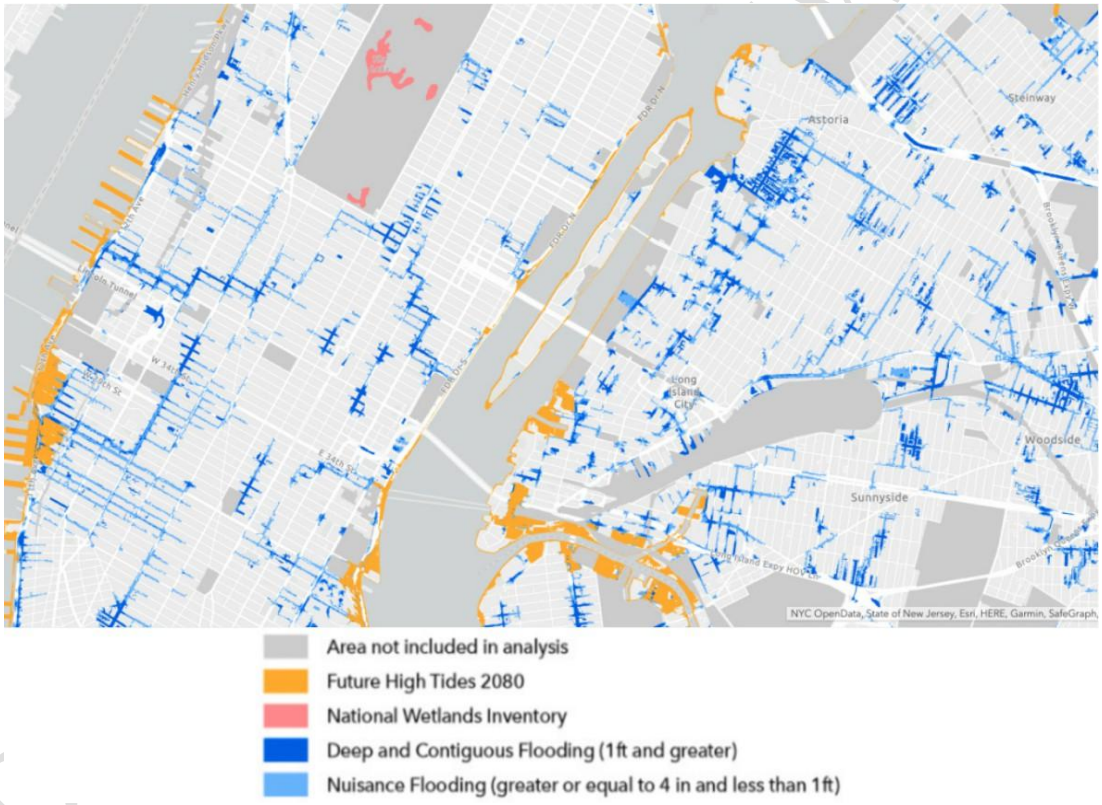

Figure 6: A selection of the Stormwater Flood Map from the City of New York Stormwater Resiliency Plan. It is important to note that the model only takes into account ground-level flooding across the city.

Geospatial Analysis in ArcGIS

An individual shapefile for each of the four redlining grades of each of the five boroughs were generated, yielding a total of twenty separate boundaries. Since the project is only focused on ground-level flooding, all buildings were masked out of the difference layer using a footprint shapefile from the New York City Department of Information Technology and Telecommunications. In effect, all water pixels detected from rooftops were removed from the analysis, allowing the results to focus specifically on flooding that impacted people most directly. For each of the twenty shapefiles, a raster calculation was performed to compute the total amount of pixels identified as flooded areas. From there, the proportion of pixels identified as flooded to the total amount of pixels were calculated for each redlining grade.

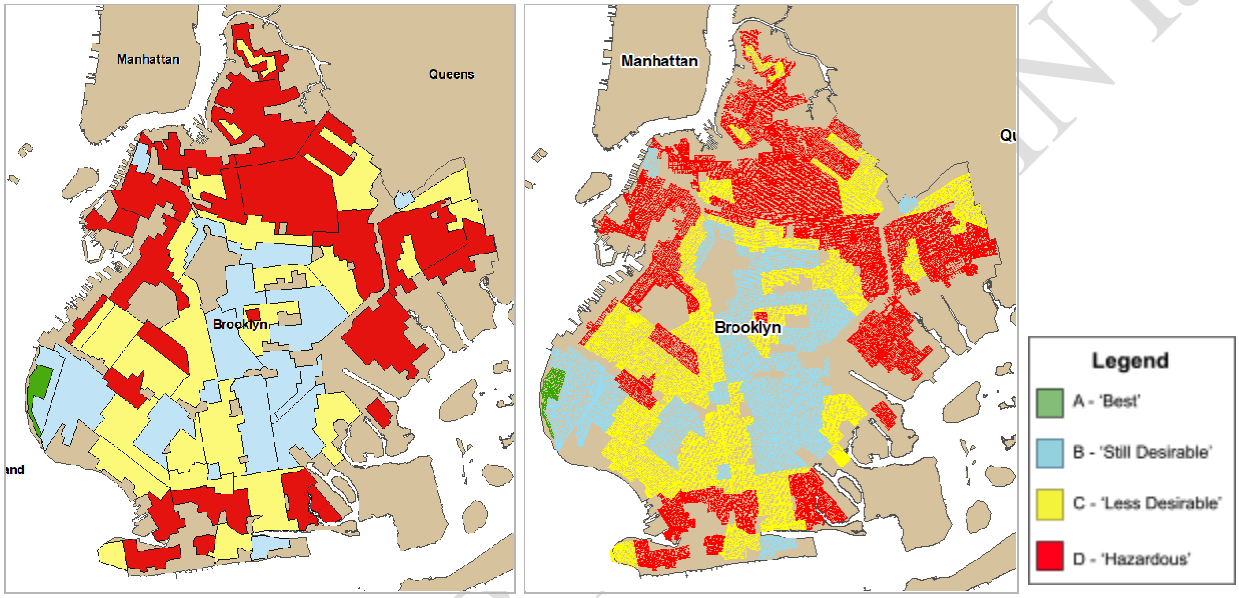

Figure 7: HOLC graded areas in the borough of Brooklyn both before building footprints were removed (left), and after building footprints were removed (right) using the 2D Building Footprints provided by the New York City Department of Information Technology and Telecommunications.

3. Results

Current Flood Risk

The percentages of each redlining grade across New York City for each of the six flood images are displayed in Figure 8. For all of the dates, the "Hazardous" neighborhoods consistently had the highest percentage of flooded streets, while the "Best" neighborhoods consistently had the lowest percentage of flooded streets.

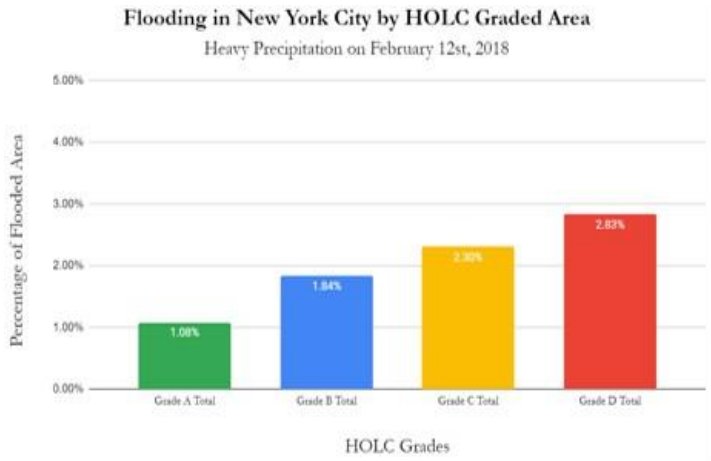

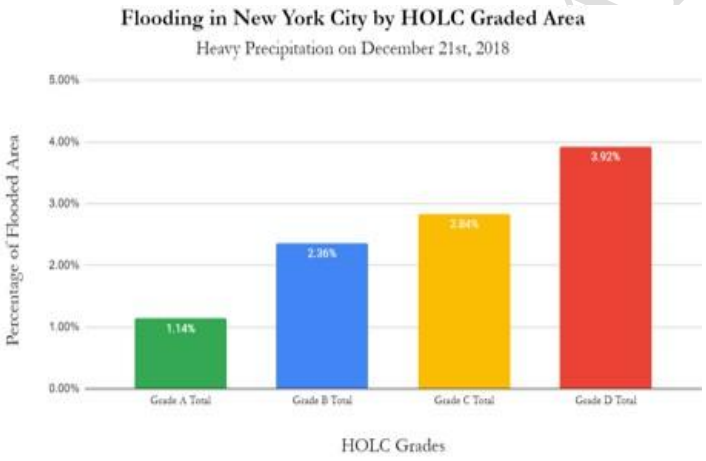

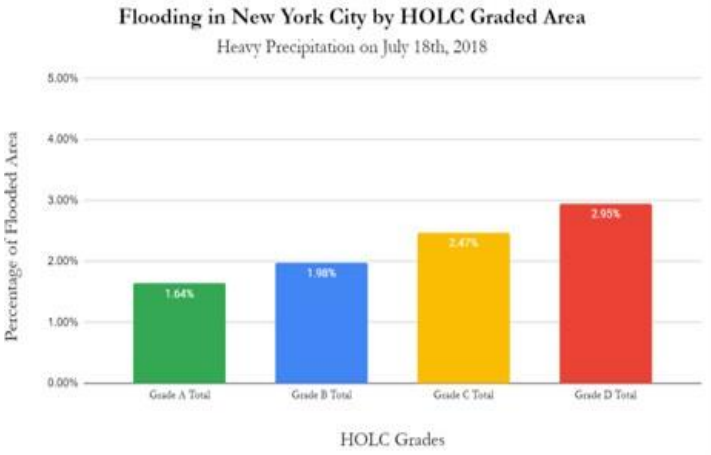

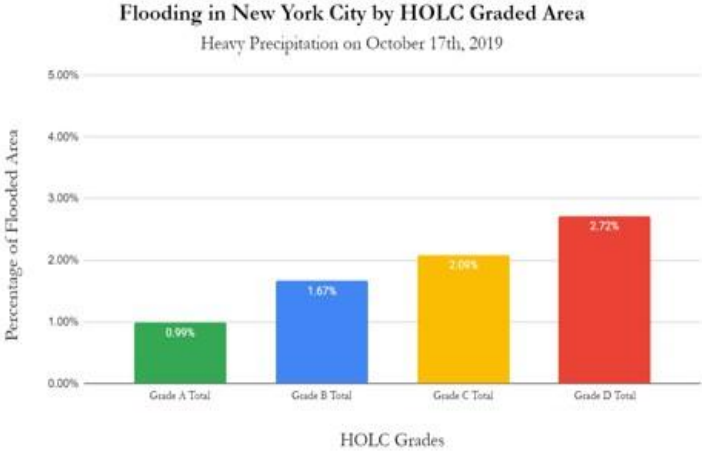

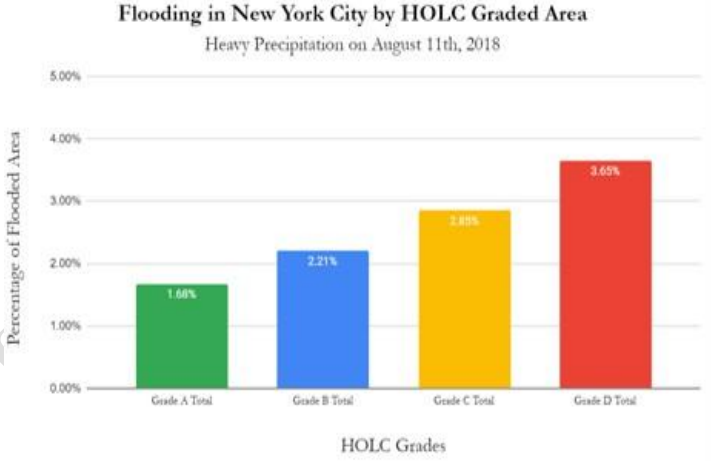

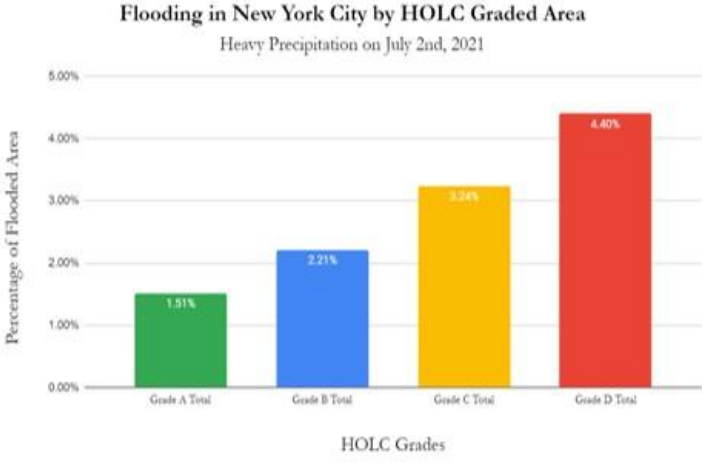

Date	Percentage of Flooded Pixels			
	Grade A	Grade B	Grade C	Grade D
02/12/18	1.08%	1.84%	2.30%	2.83%
07/18/18	1.64%	1.98%	2.47%	2.95%
08/11/18	1.68%	2.21%	2.85%	3.65%
12/21/18	1.14%	2.36%	2.84%	3.92%
10/17/19	0.99%	1.67%	2.09%	2.72%
07/02/21	1.51%	2.21%	3.24%	4.40%

Figure 8: The percentage of flooded pixels for each redlining grade for six flood event days (February 12th, 2018; July 18th, 2018; August 11th, 2018; December 21st, 2018; October 17th; 2019; July 2nd, 2021). The t-value is -6.22107 and the p-value is < 0.00001 when comparing the proportion of flooding in the "Hazardous" and "Best" neighborhoods, indicating that the results for the present-day flooding analysis are statistically significant.

Future Flood Risk

The percentages of each redlining grade across New York City within areas predicted to face moderate and extreme floods in the future are shown in Figure 9. The "Hazardous" neighborhoods have the highest percentage of future flood exposure for both the moderate and extreme scenarios, whereas the "Best" neighborhoods have the lowest percentage of street surface area predicted to experience moderate or extreme flooding.

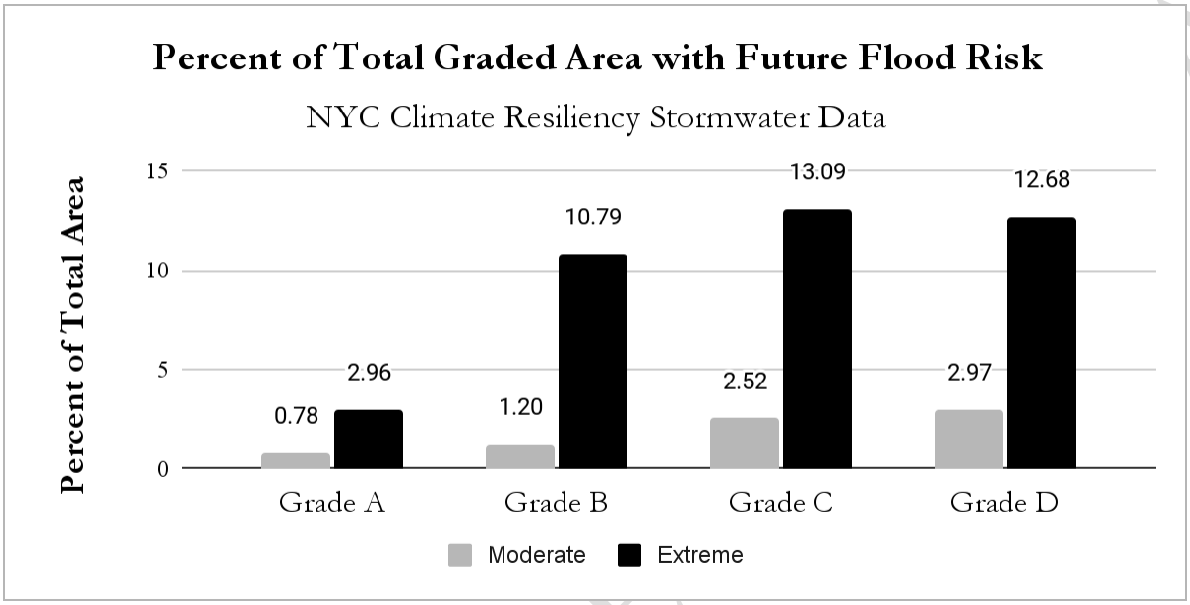

Figure 9: The percentage of flooded pixels for each redlining grade for future flood risk based on the New York City Climate Resiliency Stormwater Data. The t-value is -2.71527 and the p-value is 0.013221 when comparing the proportion of moderate future flooding in the "Hazardous" and "Best" neighborhoods. The t-value is -3.72365 and the p-value is 0.00292 when comparing the proportion of extreme future flooding in the "Hazardous" and "Best" neighborhoods. Since $p < 0.05$ for both scenarios, the results for the future flooding analysis are considered to be statistically significant.

Socioeconomic Status and Criminal Offenses

In a supplementary analysis, the flooding data for New York City was applied to determine whether there was a positive or negative relationship between the percentage of flooded pixels in a given area and the following three variables: Social Vulnerability Index, Median Household Income, and Crimes Reported.

Relationship Between Percentage of Flooded Pixels and Social Vulnerability Index

y = 0.36845 + 638.40841x

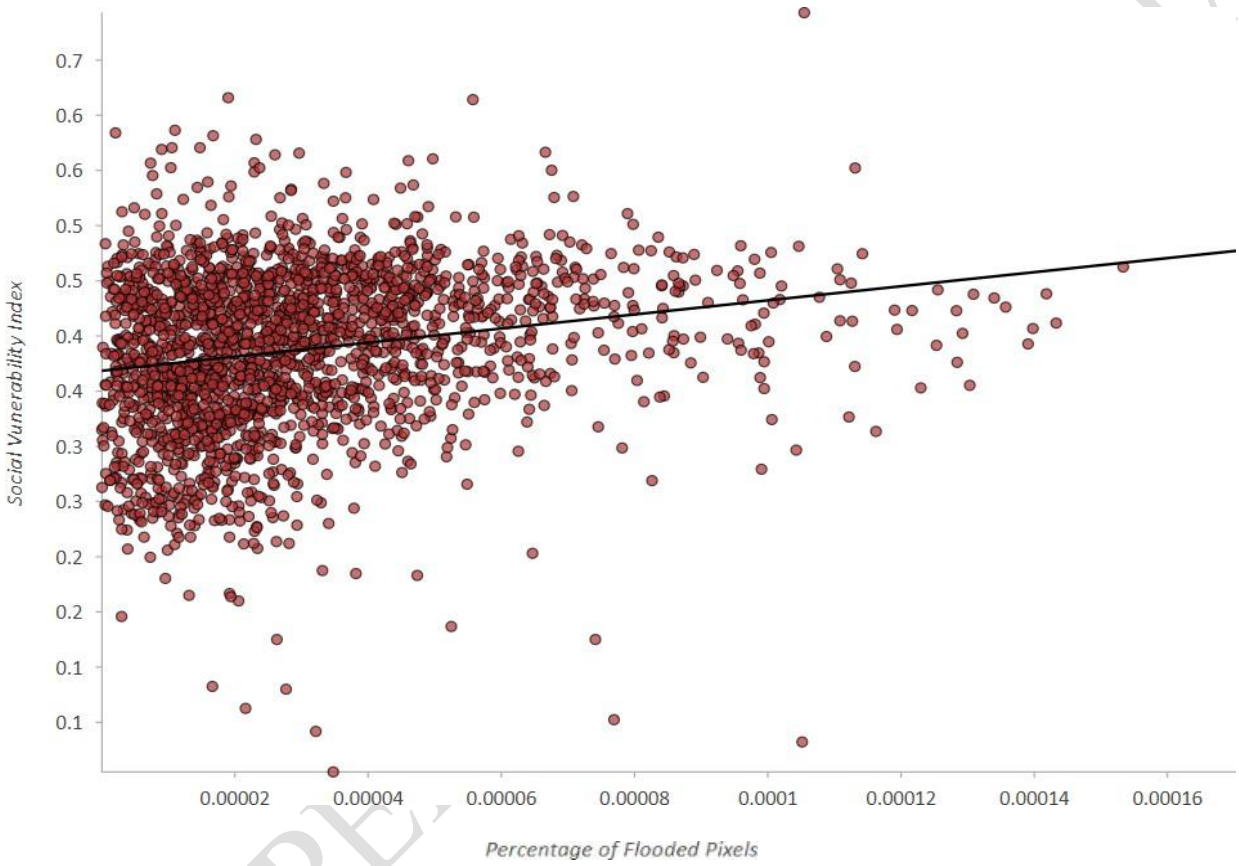

Figure 10: The relationship between the percentage of flooded pixels in New York City Census Tracts and Social Vulnerability Index. Based on data generated by the Regional Plan Association, the Social Vulnerability Index was created to reflect an individual's vulnerability to disasters by taking an average of eight variables: child care, elder care, financial restrictions, language barriers, social structure, housing density, housing uncertainty, and evacuation aid. For the Social Vulnerability Index, 0 represents the least vulnerable populations and 1 represents the most vulnerable populations (Regional Plan Association, 2015).

Relationship Between Percentage of Flooded Pixels and Median Household Income

y = 65127.42184 - 43620425.97643x

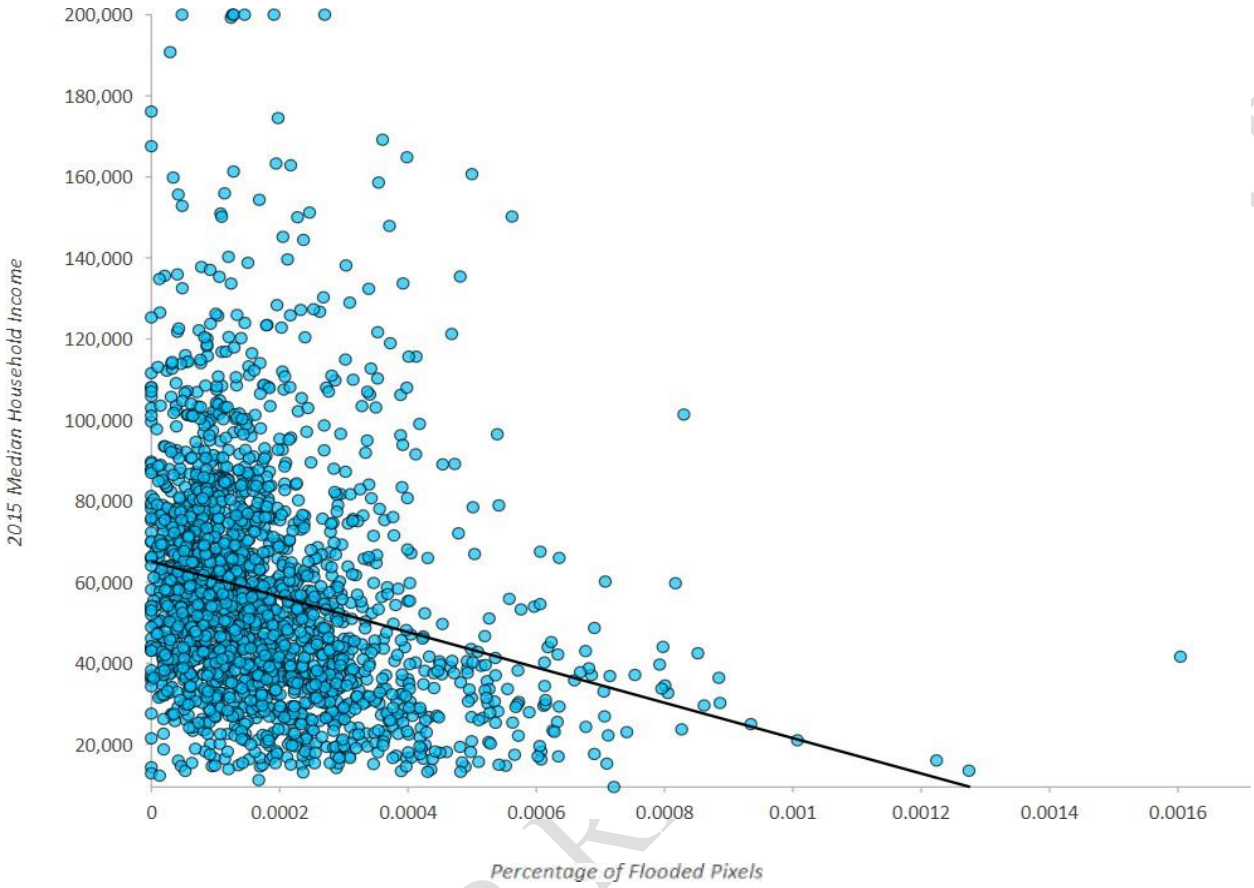

Figure 11: The relationship between the percentage of flooded pixels in New York City Census Tracts and Median Household Income. The income data employed in this analysis was collected by the United States Census Bureau.

Relationship Between Percentage of Flooded Pixels and Crimes Reported
y = 102.76417 + 252434.42524x

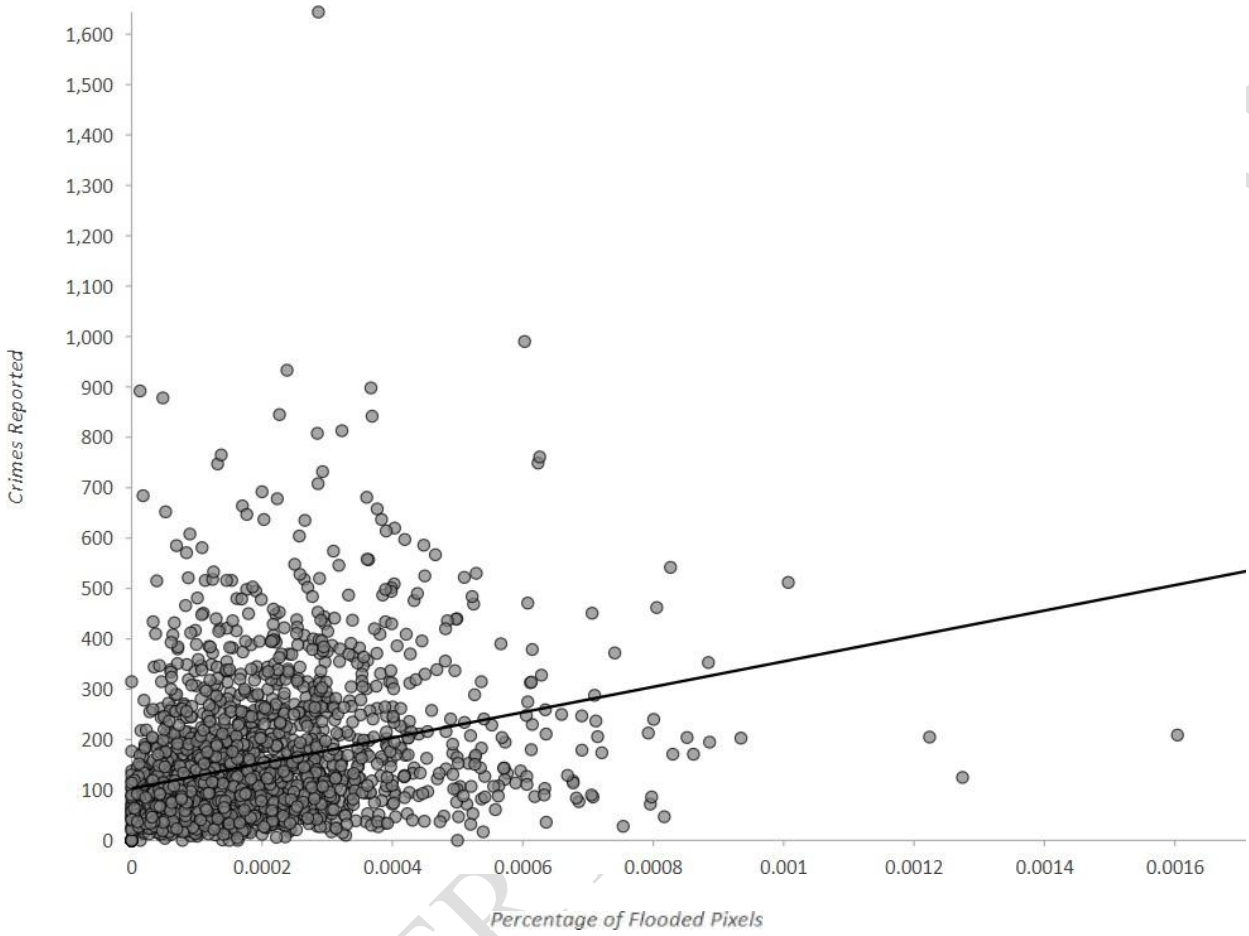

Figure 12: The relationship between the percentage of flooded pixels in New York City Census Tracts and Crimes Reported. Utilizing public complaint information collected by the New York City Police Department, the dataset includes all valid felony, misdemeanor, and violation crimes reported to the police beginning from November 2018 until October 2021 (New York City Police Department, 2021).

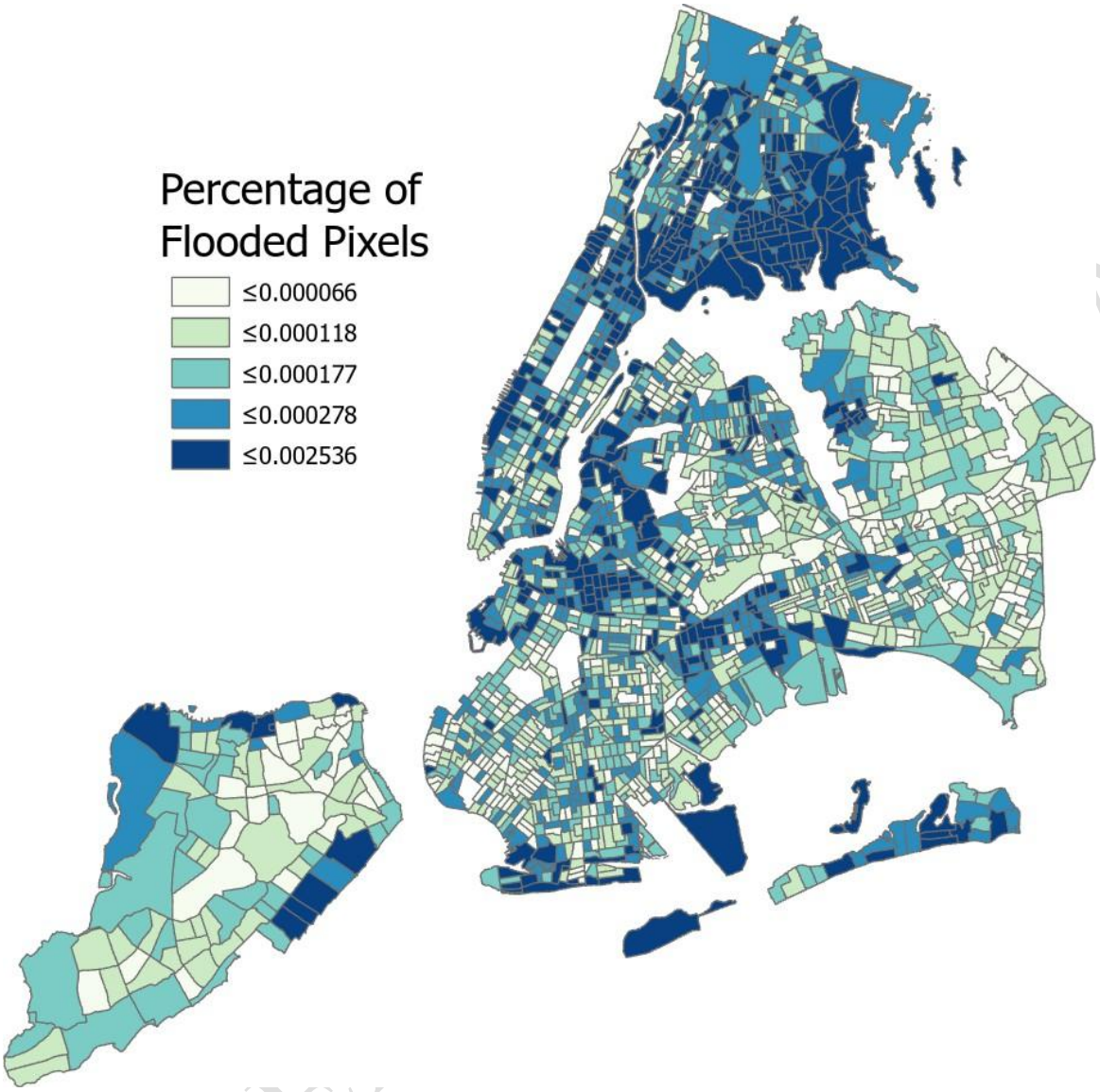

Figure 13: The spatial distribution of current flooding risk in New York City based on the percentage of flooded pixels in each Census Tract. Areas with the greatest amount of flooding, such as the South Bronx, generally correspond with areas that were graded "Hazardous" or "Definitely Declining."

4. Discussion and Conclusion

Climate Resiliency Planning

Currently, more than half of the world's population live in cities, with the amount projected to increase to two-thirds by 2050 (Rosenzweig et al., 2018). As a result, the concentration of people and infrastructure in urban areas makes cities particularly vulnerable to the impacts of climate change. Given New York City's large population density, the impact of stronger weather events is projected to cause several hundred billions of dollars in infrastructure damage, including the destruction of roads, airports, electricity supply, water supply, and sewage disposal systems if sufficient climate adaptation strategies are not enforced (Solecki 2012).

In addition to widespread economic damage, flooding events can also have major consequences on public health. First and foremost, death and injury can occur due to high stream flow velocity. Contact with water can lead to respiratory diseases, hypothermia, and cardiac arrest. Contact with polluted water can lead to wound infections, conjunctivitis, gastrointestinal illnesses, ear infections, nose infections, throat infections, and severe waterborne diseases. Even ill health in the form of physical and emotional stress may persist for months to years following a flood, causing an increase of susceptibility to psychosocial disturbances and cardiovascular incidents (World Health Organization, 2002).

In general, the ability of a community to recover from extreme weather events is determined by the risk of exposure and access to the resources needed for recovery (Hampstead et al., 2021). Therefore, the flood detection algorithm discussed in this paper is exceptionably applicable, as it can be utilized to determine the areas that are most vulnerable to current flooding events.

New York City especially requires updates to its current climate resiliency plan. Due to the damages from flooding that ensued because of Hurricane Ida, legislation has recently been approved requiring the city government to make a comprehensive plan that will protect every neighborhood from the threats of climate change (Barnard, 2021). Now that the most at-risk locations for urban flooding can be easily identified with my Google Earth Engine algorithm, communities can better protect themselves for future events.

Regarding flood prevention, protection, and preparedness specifically, there are a multitude of solutions currently available that can minimize damages to both human health and the economy through a combination of gray infrastructure and green infrastructure. Gray infrastructure practices that protect against flooding in urban settings include the construction of channels, storm surge defenses, and barriers. Correspondingly, green infrastructure practices that enhance infiltration include the expansion of natural flood plains, urban green spaces, rain gardens, bioswales, and permeable pavements (Environmental Protection Agency). Again, the results from my methodology allow policymakers to target the neighborhoods where these flood adaptation measures would have the greatest positive impact.

Environmental Racism

The resilience approach for climate adaptation requires collating the characteristic features of adaptation measures with an emphasis on taking into account multiple perspectives (Radhakrishnan et al., 2017). For this reason, scientists, policymakers, urban stakeholders, and

everyday citizens have to work in conjunction with one another to determine the best plan forward for communities combating climate change. In addition to detecting areas most prone to flooding with the use of remote sensing, the results from this paper have important implications for how to approach climate resiliency planning in a more equitable manner.

Out of the four redlining categories, "Hazardous" neighborhoods are consistently the most vulnerable to flooding events. In fact, neighborhoods identified as "Hazardous" are around twice as likely to experience chronic flooding today than areas identified as "Best." The results are even more desolate in regards to vulnerability for future flooding events, with neighborhoods identified as "Hazardous" being more than four times as likely to be impacted by extreme future flooding than areas identified as "Best." Furthermore, neighborhoods containing a higher percentage of flooded areas are more vulnerable on the Social Vulnerability Index, have lower median household incomes, and experience more criminal activity compared to neighborhoods containing a lower percentage of flooded areas.

By taking environmental justice into account for climate resiliency planning, communities can better understand pre-existing inequities in our society and how the impacts of climate change can continue to exacerbate these devastating effects.

5. References

Acharya, Tri, et al. “Evaluation of Water Indices for Surface Water Extraction in a Landsat 8 Scene of Nepal.” *Sensors*, vol. 18, no. 8, 7 Aug. 2018, p. 2580., https://doi.org/10.3390/s18082580.

Barnard, Anne. “Ida Flooding Deaths Push Council to Demand Climate Change Plan for New York.” *The New York Times*, The New York Times, 7 Oct. 2021, https://www.nytimes.com/2021/10/07/nyregion/nyc-storm-flood-preparation-plan.html.

Fishback, Price, et al. “Race, Risk, and the Emergence of Federal Redlining.” *National Bureau of Economic Research*, Nov. 2020, https://doi.org/10.3386/w28146.

González, Jorge E., et al. “New York City Panel on Climate Change 2019 Report Chapter 2: New Methods for Assessing Extreme Temperatures, Heavy Downpours, and Drought.” *Annals of the New York Academy of Sciences*, vol. 1439, no. 1, 15 Mar. 2019, pp. 30–70., https://doi.org/10.1111/nyas.14007.

Hamstead Zoé A., et al. *Resilient Urban Futures*. Springer International Publishing, 2021.

Hoffman, Jeremy S., et al. “The Effects of Historical Housing Policies on Resident Exposure to Intra-Urban Heat: A Study of 108 US Urban Areas.” *Climate*, vol. 8, no. 1, ser. 12, 13 Jan. 2020. *12*, https://doi.org/10.3390/cli8010012.

Horton, Radley, et al. “New York City Panel on Climate Change 2015 Report Chapter 1: Climate Observations and Projections.” *Annals of the New York Academy of Sciences*, vol. 1336, no. 1, 2015, pp. 18–35., https://doi.org/10.1111/nyas.12586.

Lerner, Michele. “One Home, a Lifetime of Impact.” *The Washington Post*, WP Company, 23 July 2020, https://www.washingtonpost.com/business/2020/07/23/black-homeownership-gap.

Li, Dongying, et al. “Modeling the Relationships between Historical Redlining, Urban Heat, and Heat-Related Emergency Department Visits: An Examination of 11 Texas Cities.” *Environment and Planning B: Urban Analytics and City Science*, 23 Aug. 2021, https://doi.org/10.1177/23998083211039854.

“Manage Flood Risk.” *EPA*, Environmental Protection Agency, https://www.epa.gov/green-infrastructure/manage-flood-risk.

National Climate Assessment (2018). Fourth National Climate Assessment. Volume II: Impacts, Risks, and Adaptation in the United States

Nelson, R.K., Winling, L., Marciano, R., Connolly, N. “Mapping Inequality,” American Panorama, ed. Robert K. Nelson and Edward L. Ayers, accessed July 14, 2021, https://dsl.richmond.edu/panorama/redlining/[YOUR VIEW].

"NYPD Complaint Data Current (Year to Date)." *NYC Open Data*, New York City Police Department, 19 Oct. 2021, https://data.cityofnewyork.us/Public-Safety/NYPD-Complaint-Data-Current-Year-To-Date-/5uac-w243.

Pielke, Roger A., and Mary W. Downton. "Precipitation and Damaging Floods: Trends in the United States, 1932–97." *Journal of Climate*, vol. 13, no. 20, 15 Oct. 2000, pp. 3625–3637., https://doi.org/10.1175/1520-0442(2000)013<3625:padfti>2.0.co;2.

Radhakrishnan, Mohanasundar, et al. "Structuring Climate Adaptation through Multiple Perspectives: Framework and Case Study on Flood Risk Management." *Water*, vol. 9, no. 2, 19 Feb. 2017, p. 129., https://doi.org/10.3390/w9020129.

Rosenzweig, Cynthia, et al. "Pathways to Urban Transformation." *Climate Change and Cities: Second Assessment Report of the Urban Climate Change Research Network*, Cambridge University Press, New York, New York, 2018, pp. 3–26.

Saverino, Kelly C., et al. "Thermal Inequity in Richmond, VA: The Effect of an Unjust Evolution of the Urban Landscape on Urban Heat Islands." *Sustainability*, vol. 13, no. 3, 1 Feb. 2021, p. 1511., https://doi.org/10.3390/su13031511.

Schumann, Guy, et al. "Progress in Integration of Remote Sensing–Derived Flood Extent and Stage Data and Hydraulic Models." *Reviews of Geophysics*, vol. 47, no. 4, 12 Nov. 2009, https://doi.org/10.1029/2008rg000274.

"Social Vulnerability Index." *BetaNYC Community Data Portal*, Regional Plan Association, 2 Mar. 2015, https://data.beta.nyc/en/dataset/social-vulnerability-index.

Solecki, William. "Urban Environmental Challenges and Climate Change Action in New York City." *Environment and Urbanization*, vol. 24, no. 2, Oct. 2012, pp. 557–573., https://doi.org/10.1177/0956247812456472.

Wilson, Bev. "Urban Heat Management and the Legacy of Redlining." *Journal of the American Planning Association*, vol. 86, no. 4, 22 May 2020, pp. 443–457., https://doi.org/10.1080/01944363.2020.1759127.

World Health Organization, 2002, pp. 1–49, *Floods: Climate Change and Adaptation Strategies for Human Health*.

Xu, Hanqiu. "Modification of Normalised Difference Water Index (NDWI) to Enhance Open Water Features in Remotely Sensed Imagery." *International Journal of Remote Sensing*, vol. 27, no. 14, 22 Jan. 2006, pp. 3025–3033., https://doi.org/10.1080/01431160600589179.